Above-ground biomass estimation of arable crops using UAV-based SfM photogrammetry

Methods of estimating the total amount of above-ground biomass (AGB) in crop fields are generally based on labourious, random, and destructive in situ sampling. This study proposes a methodology for estimating herbaceous crop biomass using conventional optical cameras and structure from motion (SfM) photogrammetry. The proposed method is based on the determination of volumes according to the difference between a digital terrain model (DTM) and digital surface model (DSM) of vegetative cover. A density factor was calibrated based on a subset of destructive random samples to relate the volume and biomass and efficiently quantify the total AGB. In all cases, RMSE Z values less than 0.23 m were obtained for the DTM-DSM coupling. Biomass field data confirmed the goodness of fit of the yield-biomass estimation (R^2=0,88 and 1,12 kg/ha) mainly in plots with uniform vegetation coverage. Furthermore, the method was demonstrated to be scalable to multiple platform types and sensors.

Keywords: DSM; DTM; drone; AGB; volume determination; VHR image

To cite this article: ML. Gil-Docampo, M. Arza-García, J. Ortiz-Sanz, S. Martínez-Rodríguez, JL. Marcos-Robles & LF. Sánchez-Sastre (2018) Above-ground biomass estimation of arable crops using UAV-based SfM photogrammetry, Geocarto International, DOI: 10.1080/10106049.2018.1552322

1 Introduction

Crop monitoring is an essential practice in smart farming. In addition to knowledge of natural factors, such as water availability or soil quality, knowledge of the health status of a field and nutrient inputs can assist in estimating the predicted yield. A rapid, economical, and quantitative estimation of biophysical variables, such as biomass, is important for accessibility risk management, global markets, and policy and decision making (Becker-Reshef et al. 2010). Field methods provide consistent techniques for the quantification of biomass but are usually expensive and based on destructive sampling. Although these methods can be accurate, they are labour intensive and susceptible to undersampling in spatially heterogeneous ecosystems (Cunliffe et al. 2016).

Remote sensing methods can be integrated with field assessments to produce the information needed to estimate above-ground biomass (AGB) over a wide range of scales. The advantages of biomass estimation using these methods include the possibility of obtaining measurements for each location, the ability to collect data in areas that are difficult to access from the ground, the speed at which data can be captured and processed, and the relatively low cost of many remote sensors (Bortolot & Wynne 2005).

Traditionally, the remote sensors used to detect vegetation cover are active or passive (Qazi et al. 2017). Specifically, the methods that have been widely used to estimate biomass are passive optical systems of high and medium resolution (Solberg et al. 2009), active radar systems (Koch 2010; Feng et al. 2018), and light detection and ranging (LIDAR) sensors (Vazirabad & Karslioglu 2011; Eitel et al. 2016). Using multiple regression techniques, kNN (k-nearest neighbors) classification or neural networks, it is possible to directly relate the signal response captured by the sensor and the quantity of AGB (Wu et al. 2016; Yang et al. 2018). Although these methods reduce the dependency on in situ sampling, some in-field data are often required to accurately relate the signal obtained by the sensor with the structural properties of plants (e.g., height, weight, density, etc.). These relationships, which consider plant allometry, can be further calibrated and generalized for specific species.

To cite this article: ML. Gil-Docampo, M. Arza-García, J. Ortiz-Sanz, S. Martínez-Rodríguez, JL. Marcos-Robles & LF. Sánchez-Sastre (2018) Above-ground biomass estimation of arable crops using UAV-based SfM photogrammetry, Geocarto International, DOI: 10.1080/10106049.2018.1552322

The systems based on passive remote sensing depend on the variability of the spectral responses of vegetation in the visible and near-infrared regions. Widely used indices, such as the normalized difference vegetation index (NDVI), have also been empirically correlated with biomass (Goswami et al. 2015; Zhu & Liu 2015; Fern et al. 2018). However, the ability of some active sensors, such as LIDAR, to penetrate vegetation cover and obtain precise crop metrics for height, density and volume represents a major advancement in biomass studies. Active sensors have the added benefit of not relying on ambient lighting conditions, and they allow for greater flexibility in usage, particularly at the agricultural level (Liu et al. 2017). Recently, LIDAR use has been strengthened by the development of smaller and lighter devices that can be transported via unmanned aerial vehicle (UAV) systems. Moreover, LIDAR sensors have experienced a significant reduction in cost, although they are significantly most expensive than optical systems.

Photogrammetric techniques are undoubtedly more economically affordable than those discussed above. However, these techniques do not have a long history in the quantification of vegetation metrics due to the problems that vegetation cover generates in the correlation process (e.g., difficulty in identifying homologous points and shaded areas) and the inability to penetrate dense vegetation canopies (Harwin & Lucieer 2012; Rosnell & Honkavaara 2012). However, photogrammetric techniques have undergone recent improvements with the implementation of automated image correlation (AIC) techniques. These techniques achieve much higher levels of precision and automation than those of traditional digital photogrammetry. So-called automated digital photogrammetry, together with the SfM (structure from motion) and DMVR (dense multiview 3D reconstruction) algorithms, can be used to produce 3D models of more complex and heterogeneous spatial structures, such as vegetation, with remarkable improvements in precision (Koutsoudis et al. 2014).

In addition, the use of UAVs as elevated platforms for sensors has become popular in precision agriculture. Compared with airborne aerial surveys, UAVs are much more flexible and efficient in terms of functionality. For example, UAVs are increasingly used to study crops, such as in the monitoring and mapping of grasslands (Lu & He 2017), assessing actual crop conditions and parameters such as nitrogen

To cite this article: ML. Gil-Docampo, M. Arza-García, J. Ortiz-Sanz, S. Martínez-Rodríguez, JL. Marcos-Robles & LF. Sánchez-Sastre (2018) Above-ground biomass estimation of arable crops using UAV-based SfM photogrammetry, Geocarto International, DOI: 10.1080/10106049.2018.1552322

(Liu et al. 2017), and estimating and predicting plant heights and volumes (Bendig et al. 2014; Geipel et al. 2014; Iqbal et al. 2017). The compatibility of these platforms with conventional digital cameras and the ability to perform semi-autonomous or autonomous flights result in considerable ease of use. In addition, costs are significantly lower compared with those of traditional manned flights (Nex & Remondino 2014; Mondino & Gajetti 2017). In this respect, UAV technology constitutes an appropriate support mechanism for aerial photogrammetry in the mass capture of high-resolution images.

This work proposes a methodology based on the use of SfM software for estimating AGB by defining a density factor (DF) to link field data with UAV photogrammetry-derived digital surface models (DSMs). We identify two important questions: (1) is the method scalable to multiple platforms (both fixed-wing and rotary wing platforms) and sensors, and (2) is the method a valid approach for AGB estimation?

2 Materials and methods

2.1 AGB estimation workflow

The crop volume is highly correlated with the AGB (Walter et al. 2018). However, estimating the quantity of AGB based exclusively on the crop volume, with a reasonable level of accuracy, is not possible if plant allometry (i.e., relationships based on plant shape, height, size, age or structure) is ignored. However, robust allometric relations are difficult to establish and require intense sampling and specific studies of specific plant varieties (Cooper et al. 2017). Thus, we propose a semi-automated workflow for AGB estimation based on the crop density (Fig. 1). This approach assumes an equal distribution of vegetation density across the plot and therefore does not require further allometric information. In-field crop sampling allows for the calibration of a DF that relates the weight of the field sample to the volume of vegetation at each sampling point, and thus, the relation between the crop volume and AGB can easily be generalized for the entire plot.

Similar to LIDAR, SfM photogrammetry can provide high-fidelity point clouds or derived triangulated DSMs for a crop surface. However, in contrast to laser methods, SfM cannot fully penetrate crop canopies. Therefore, to compute volumes, it is necessary to employ a surface difference method with an auxiliary

To cite this article: ML. Gil-Docampo, M. Arza-García, J. Ortiz-Sanz, S. Martínez-Rodríguez, JL. Marcos-Robles & LF. Sánchez-Sastre (2018) Above-ground biomass estimation of arable crops using UAV-based SfM photogrammetry, Geocarto International, DOI: 10.1080/10106049.2018.1552322

DTM and compute the volumes as the difference between bare-field digital model (DTM) and that with crops (DSM). The source of the DTM can be a previous flight over a bare field or other sources, such as a public geodata repository. Although more homogeneous data can simplify the adjustment of the z-coordinate (DTM from a previous drone flight before the establishment of a plantation), the DTM employed in this work was obtained from the National Plan of Aerial Orthophotography (PNOA) of the Spanish National Geographic Institute (http://www.ign.es/). This DTM (RMSEx, y< 0.4 m and RMSE z<1 m) is a 5x5 m grid derived from the national LIDAR flight. The hybrid coupling approach (different sources for the DTM/DSM) is a common method applied in photogrammetric biomass studies, particularly in the forestry field (Wong et al. 2015; Kachamba et al. 2016), in which having different flight periods is meaningless. This coupling requires a procedure to verify the accuracy of the adjustment between models.

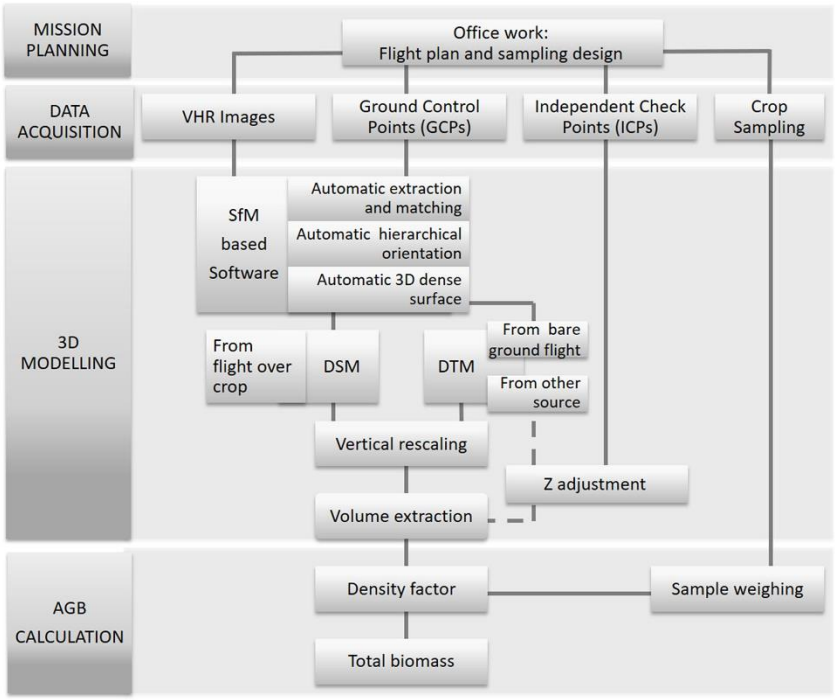

Fig. 1. Workflow for AGB determination using close-range photogrammetry

2.2 Study site and field campaigns

A study of the application of the proposed methodology was conducted in three plots with low fertility and semiarid soils located in northcentral Spain (Fig. 2) planted with different herbaceous crops (*Vicia sativa*, *Triticum sativum*, *Secale cereale*, triticale, and *Medicago sativa*). Two experimental plots (Ayoó de Vidriales [42º07´N, 6º 06´W, Zamora] and Soto de Cerrato [41º56´N, 4º26´W, Palencia]) and a commercial plot in San Mateo de Gallego (41º48N, 0º45´W, Zaragoza) were used to test the method. The surfaces in each case are specified in Table 1. The study was performed in two campaigns in June (2013 and 2016).

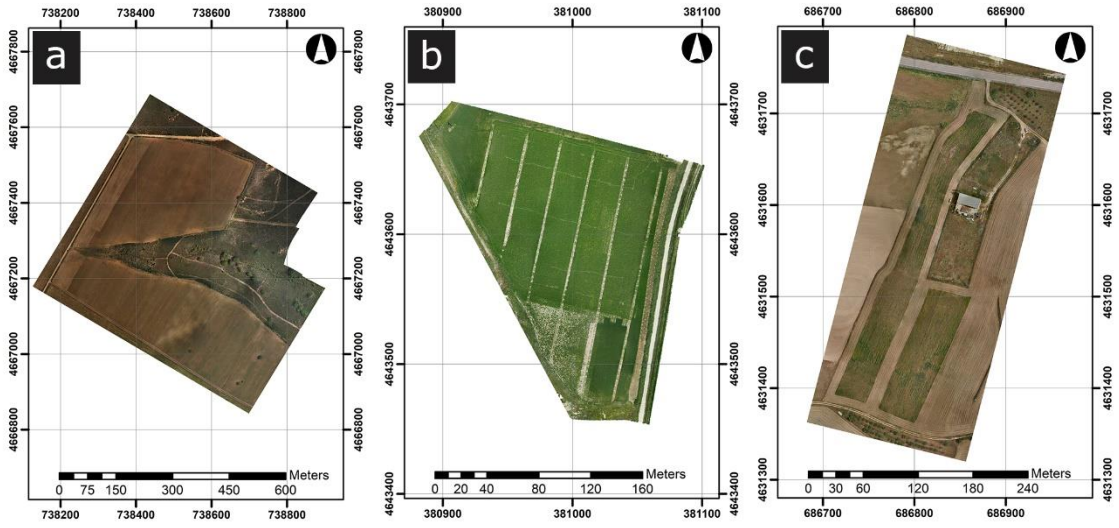

Fig. 2. Location and overview of research plots: a) Ayoó de Vidriales; b) Soto de Cerrato and c) San Mateo de Gallego

During crop sampling, simple random sampling was implemented, and field samples were obtained immediately after each photogrammetric flight. For each random sample point, a ring with a known surface area (0.25 m²) was thrown, and the aerial parts of plants inside the ring were harvested. The roots were clipped, and the samples were cleaned and weighed separately on the same day to obtain a fresh biomass measurement. After drying the samples at 70 °C for 5 days, each sample was weighed again separately to obtain dry biomass values.

To cite this article: ML. Gil-Docampo, M. Arza-García, J. Ortiz-Sanz, S. Martínez-Rodríguez, JL. Marcos-Robles & LF. Sánchez-Sastre (2018) Above-ground biomass estimation of arable crops using UAV-based SfM photogrammetry, Geocarto International, DOI: 10.1080/10106049.2018.1552322

2.3 Generation of high-resolution DSMs for crops

The workflow for DSM generation is commonly used for any 3D mapping procedure with UAV-based imagery and includes mission planning, data acquisition, and 3D modelling (Nex & Remondino 2014).

2.3.1 Mission planning

Flight planning is the most important step in the creation of a high-quality 3D model and can lead to accurate volume quantification and accurate AGB estimation. The planning of the mission must be based on the ground sample distance (GSD) and the parameters of the camera (e.g., the focal length and sensor pixel size). From these fixed parameters and the desired GSD value, the flight altitude can be determined (flight height = GSD x focal length / pixel size). The overlap between photographs varies depending on the purpose of the mission. In flights for which precise results are required, a high degree of longitudinal and transversal overlap (e.g., 80-70%) is needed to guarantee the accuracy of the model. Each point of the scene must appear in a larger number of photographs to refine the position of the point via data redundancy. The waypoints that the UAV follows during a mission and the positions of the shots are automatically calculated based on these parameters.

Flight planning software can be used to set up automatic missions based on the creation of the waypoints that the autopilot is able to follow. Generally, every company provides unique planning solutions (e.g., U-see (Airelectronics), eMotion (Sensefly), mdCockpit (Microdrones), Ground Station -GS- (DJI), etc.), but many other solutions can be used with multiple platforms (e.g., UGCS, Mission Planner, DroneDeploy, etc.). These solutions can be used for automatic mission planning, flight monitoring, real-time telemetric data visualization and capturing video.

2.3.2 Data acquisition

To cite this article: ML. Gil-Docampo, M. Arza-García, J. Ortiz-Sanz, S. Martínez-Rodríguez, JL. Marcos-Robles & LF. Sánchez-Sastre (2018) Above-ground biomass estimation of arable crops using UAV-based SfM photogrammetry, Geocarto International, DOI: 10.1080/10106049.2018.1552322

VHR images were taken using vertical take-off and landing (VTOL) and fixed-wing platforms (Table 1). Despite offering low flight autonomy, VTOL platforms allow greater camera stabilization and can fly at a lower speed compared to fixed-wing UAVs. In all cases, the UAV itself was responsible for automatically operating the camera based on the initial flight plan.

Table 1. Data acquisition equipment used for each plot

Flight Campaign	Name	Surface (m^2)	Drone	Camera (focal)
Jun. 2013	Soto de Cerrato	13,7	[Multirotor] MD4-1000 (Microdrones, Siegen, Germany)	Olympus E-P3 (17 mm) - 12.3 MP
	San Mateo de Gallego	17,7		
	Ayoó de Vidriales	226,9		
Jun. 2016	Soto de Cerrato	21,7	[Multirotor] Oktokopter XL (Mikrokopter, Moormerland, Germany)	Olympus E-P3 (17 mm) - 12.3 MP
	San Mateo de Gallego	50,7	[Fixed-wing] Skywalker Kit (Airelectronics, Madrid, Spain)	Canon PowerShot A810 (5 mm) - 16 MP
	Ayoó de Vidriales	158,0	[Fixed-wing] eBee (SenseFly, Lausanne, Switzerland)	Sony CyberShot WX500 (5 mm) -18 MP

Ground control points (GCPs) were collected in the field for the generation of terrain models using a dual-frequency static GPS receiver (Leica SR530, 3 mm+0.5 ppm min X, Y and Z). Agisoft Photoscan requires a minimum number of 3 GCPs to adjust the photogrammetric block. Although several studies have discussed this issue (Goldstein et al. 2015; Tonkin & Midgley 2016), there is no distinct accepted criterion for establishing the number of GCPs, and the choice also depends on the size of the plot. Tonkin & Midgley (2016) showed that for a particular case, 3 or 4 GCPs may result in acceptable levels of error within the quality range of the measurement source (GPS). In addition, Goldstein et al. (2015) suggested that diminishing returns occur when greater than 10 GCPs are used. The number of GCPs employed in each one of the test plots can be seen in Table 2. These points were distributed on the ground and covered the

block sides and edges of the plot. The points were defined based on highly identifiable elements in the photographs taken using the drone.

2.3.3 3D modelling

The final step in DSM generation involves (1) automatic correlation, (2) hierarchical orientation, and (3) automatic 3D dense surface extraction. These processes are carried out using photogrammetric software based on SfM algorithms, such as Photoscan (Agisoft, Saint-Petersburg). In stage (1), the software searches for common points in photographs and matches them; additionally, the position of the camera is determined for each image, and the camera calibration parameters are refined. In stage (2), a set of camera positions is formed. Based on the estimated camera positions, the program calculates depth information for each camera, and this information is combined into a single dense point cloud. In stage (3), input parameters of the SfM process are set to "High" or "Very high" in all stages, which implies that the DSMs are generated using a resolution corresponding to the original GSD.

2.4 Terrain model adjustment

A z-coordinate adjustment must be made between the two models. This adjustment procedure consists of identifying 30 homologous points without vegetation in both the DSM and the DTM. The mean value of the difference between Z_{DSM} and Z_{DTM} is used to correct the z-coordinate of the DSM and achieve precise coupling.

Once the study area has been delineated, the total vegetation volume can be determined with a surface difference method (Fig. 3). Most GIS and cartography programs, such as ArcGIS (ESRI, California), Global Mapper (Blue Marble, Maine), GRASS GIS (*Open-Source*, originally Illinois) or Sputnik GIS (Geoscan, Saint-Petersburg), incorporate automated routines or tools for volume computations between surfaces. In this study, we used the tool “Measure volume between surfaces” in Global Mapper v. 19.0.0. This software

uses the DSM (Fig. 3a) and DTM (Fig. 3b) to obtain difference maps (Fig. 3c) and compute overall volume data and statistics. Further analysis of altitudinal differences can be performed using cross-section graphs (Fig. 3d).

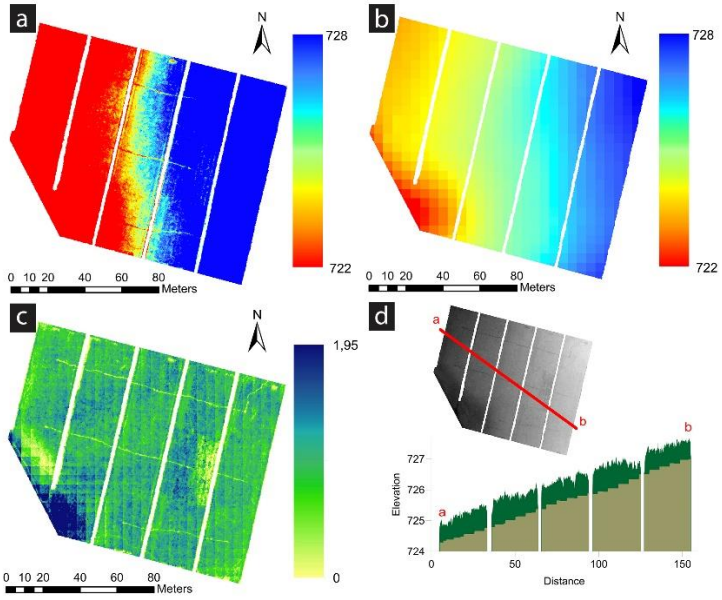

Fig. 3. Process of volume extraction for the Soto de Cerrato plot (2013): a) DSM; b) DTM; c) volume based on the difference between surfaces; and d) vertical profile across models

2.5 AGB calculation

The biomass in each plot is estimated by calculating the DF, which relates the volume per unit surface area to the weight per unit surface area (Fig. 4). This calculation is performed using biomass sampling points measured in the field. Aleatory sampling of the plot is performed with a ring, and the vegetation inside the ring is harvested and weighed.

To cite this article: ML. Gil-Docampo, M. Arza-García, J. Ortiz-Sanz, S. Martínez-Rodríguez, JL. Marcos-Robles & LF. Sánchez-Sastre (2018) Above-ground biomass estimation of arable crops using UAV-based SfM photogrammetry, Geocarto International, DOI: 10.1080/10106049.2018.1552322

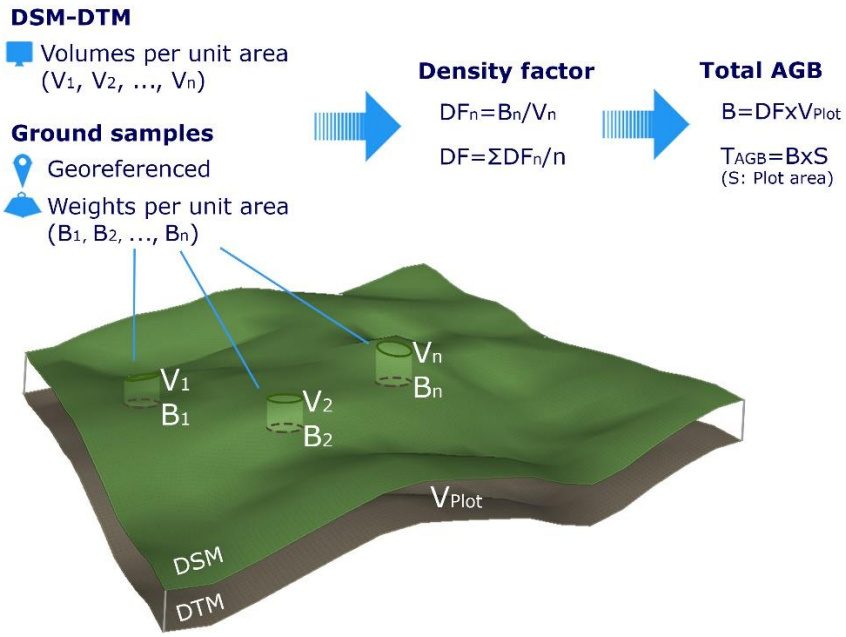

Fig. 4. AGB calculation by using the DF concept

A volume relationship between the DSM and DTM for each of the sampling points can be obtained by generating a cylindrical section from the complete model of the plot. Note that other sampling frame geometries (e.g., square or rectangular) can also be used. A DF is obtained for each point by relating the weight value of each sample to the measured volume.

$$DF = \frac{B}{V} \qquad (1)$$

where

a) *DF*: density factor (kg/m^3),

b) *B*: biomass per unit area (kg/ha), and

c) *V*: volume per unit area (m^3/ha).

Notably, the proposed DF does not represent any physical characteristics of the plot. Instead, it is a volume relationship between the digital models and the mass measured at each point during field sampling. PhotoScan calculates a larger volume if the vegetation layer is dense and a lower volume if the vegetation

layer is sparse. DF allows for the correction of these volume variations and produces an objective calculation of biomass in the remainder of the plot.

The weight values obtained for each sample are then extrapolated to the entire plot surface through the calculation of the average plot DF. Therefore, the field samples must be representative of the heterogeneity of the crop. The biomass per unit area for the plot is obtained using the following equation.

$$B = DF \times V \quad (2)$$

Additionally, the total AGB is calculated as follows:

$$T_{AGB} = B \times S \quad (3)$$

where

a) T_{AGB}: total above-ground biomass of the plot (kg),

b) B: biomass per unit area (kg/ha), and

c) S: total plot surface (ha).

3 *Results and discussion*

3.1 Scalability of the method to multiple platforms and sensors

The sensor/flying height ratio was likely the most important factor that determined the accuracy of the DSM. The flight height was adjusted for each trial to provide a 2–5 cm GSD in accordance with the camera used, the canopy height, and the homogeneity of the crop. Using high flying heights has a negative effect on the altimetric fidelity of the DSM and therefore on the accuracy of the volumetric measurements. Additionally, large along- and across-track overlaps (80% and 70%, respectively) were used.

After the first campaign, two data acquisition improvements were implemented in the second campaign. First, the pixel size (i.e., sensor)/flight height ratio was adjusted such that it did not affect the fidelity of the DSM and, consequently, the reliability of the volume measurements. The camera used in the first campaign

To cite this article: ML. Gil-Docampo, M. Arza-García, J. Ortiz-Sanz, S. Martínez-Rodríguez, JL. Marcos-Robles & LF. Sánchez-Sastre (2018) Above-ground biomass estimation of arable crops using UAV-based SfM photogrammetry, Geocarto International, DOI: 10.1080/10106049.2018.1552322

(Olympus Pen E-P3) is commonly used in aerial photogrammetry because it is lightweight, but the sensor resolution is not the best choice for this type of work. Therefore, higher resolution sensors improved the efficiency by flying at a higher flight altitude and maintaining the same resolution. Second, increasing the covered surface provided a planned safety area at the plot edges and did not compromise the overlaps at the boundaries of the plots. To increase the surface area of the flight in less time and to fly full plots, we also tested fixed-wing drones, which are more efficient than rotary wing drones in passing over the plots.

Table 2 shows that the RMSE Z value based on GCP adjustment was lower than 3.9 cm in all cases. The RMSE X and Y values were lower than 9 cm and 5 cm, respectively, except for the Ayoó de Vidriales plot during the 2013 campaign. A noticeable reduction in RMSE was observed by reducing the flight height from 161.3 m (2013 flight) to 84.7 m (2016 flight) over this plot.

Table 2. DSM accuracy statistics

Flight campaign	**Plot**	**Flight height (m)**	**GSD (m)**	**GCP**				**Z Checkpoints (DSM/DTM)**
				Num. GCPs	**RMSE X (m)**	**RMSE Y (m)**	**RMSE Z (m)**	**RMSE Z (m)**
Jun. 2013	Soto de Cerrato	66.3	0.021	8	0.057	0.051	0.039	0.099
	San Mateo de Gallego	115.9	0.037	26	0.001	0.001	0.002	0.195
	Ayoó de Vidriales	161.3	0.052	8	0.535	0.783	0.034	0.215
Jun. 2016	Soto de Cerrato	77.4	0.019	5	0.082	0.041	0.004	0.038
	San Mateo de Gallego	214	0.050	10	0.023	0.025	0.014	0.224
	Ayoó de Vidriales	84.7	0.022	11	0.009	0.010	0.002	0.051

To cite this article: ML. Gil-Docampo, M. Arza-García, J. Ortiz-Sanz, S. Martínez-Rodríguez, JL. Marcos-Robles & LF. Sánchez-Sastre (2018) Above-ground biomass estimation of arable crops using UAV-based SfM photogrammetry, Geocarto International, DOI: 10.1080/10106049.2018.1552322

The models with the highest spatial resolution were generally achieved with VTOL platforms (up to a 1.9-cm GSD for the Soto de Cerrato flight in 2016 with a flying height of 77.4 m). However, with the use of fixed-wing drones, it is possible to measure larger parcels during a single flight, thereby avoiding the need to create subplots. In addition, the cost of fixed-wing platforms is significantly lower for both field surveys (shorter flight time) and desktop work (a single 3D model covers several parcels).

Based on this methodology, various precautions must be taken throughout the process to improve the quality of the DSM. The first field campaign allowed us to modify different aspects of the equipment and procedures to increase the efficiency and reliability of the methodology. These modifications included correcting flight planning with a safety area at the edges of plots, obtaining high coverage to avoid any unforeseen problems caused by wind, and selecting a proper binomial camera/height ratio to obtain an appropriate GSD. It is advisable to use digital single-lens reflex cameras (DSLR) or mirrorless cameras with large sensors and a minimum resolution of 18 megapixels. The flying height will be less limiting if a camera with these characteristics is used because the GSD at a particular height will be smaller than the GSD of a low-performance camera. The use of these drones over large plots allows for the entire surface to be measured in a single flight and for the 3D model to be produced in one step. Although fixed-wing drones increase the performance per unit surface area, the on-board camera must be capable of capturing images of sufficient quality.

A certain deficiency was detected in the sharpness of the images captured using the Skywalker sensor. A noticeable reduction in the planned overlap of 70% and 40% for along- and across-track flights, respectively, was detected in the automatic shooting flight with the fixed-wing eBee (2016 campaign at San Mateo de Gallego) due to wind. Tailwinds in the same direction of the flight accelerated the UAV during some passes and decelerated the craft during passes in the opposite direction. However, metric checks confirmed that the generated 3D model was sufficiently accurate for the subsequent analysis. The low slope of the plot validated these values, and the importance of planning high overlaps was confirmed.

To cite this article: ML. Gil-Docampo, M. Arza-García, J. Ortiz-Sanz, S. Martínez-Rodríguez, JL. Marcos-Robles & LF. Sánchez-Sastre (2018) Above-ground biomass estimation of arable crops using UAV-based SfM photogrammetry, Geocarto International, DOI: 10.1080/10106049.2018.1552322

3.2 Validation of volume-based AGB estimation

DSM generation is almost completely automated using software and only requires operator intervention to introduce the GCPs. In this case, the resulting DSM represents the top coverage of the crop. The obtained DSM is edited to eliminate streets and other surfaces that do not correspond to the area used to estimate the crop; consequently, the real land surface from which to determine the final volume of AGB can be obtained.

The quality evaluation of coupling the DTM and DSM can be seen in Table 2. The evaluation was performed using 30 random ICPs on bare ground in each case. The results show the RMSE Z values below 0.23 m in all trials. A consistent relationship between these Z residual values and the height of each of the flights can be observed. Lacking a more accurate and detailed pre-existing DTM, improved results for the terrain model adjustment can be expected by deriving a DTM with UAV acquisition when the target field is bare (preferably using the same flight parameters and camera as used when the crop is standing). In any case, this is not a limiting factor because the determination of the volume is not an objective itself. The DF allows for the calculation of the total amount of biomass with some independence regarding DSM/DTM coupling. A hypothetical displacement of the DSM of 2 m upwards with respect to the DTM produces an increase in the volume measured by the software for both the sampling points and the total volume of the plot. This increase in volume proportionally reduces the value of the calculated DF, and the total amount of AGB remains invariant as long as the DSM-DTM difference remains positive at all points in the plot; otherwise, the positive and negative values offset and can lead to incorrect volumetric estimations.

The following tables show the results pertaining to the calculated volume (Table 3) and total biomass estimation above the soil (Table 4) for each plot in the study. The reliability and resulting confidence of these samples are limited if the sample represents a small section of the plot, which could lead to misrepresentation if the plot is not uniform (Luo et al. 2016). Additionally, the number of data samples collected in our experiment depended on the uniformity of the crop in a particular plot. However, because sampling is often destructive, there must be a balance between the number of samples and their

representativeness. Sampling and subsequent processing requires transport, drying, and manual handling, which contribute to sample loss and can be restrictive in large experiments (Jimenez-Berni et al. 2018).

Table 3. Volume results based on the difference between the DSM and DTM

Flight campaign	Plot	Crop	Uniformity of the crop	Num. crop samples	Surface (m^2)	Volume DSM-DTM (m^3)	Volume per surface unit (m^3/ha)
Jun. 2013	Soto de Cerrato	*Vicia sativa*	Medium	5	13,71	9,60	7,00
	San Mateo de Gallego	*Vicia sativa*	High	2	17,74	4,83	2,72
	Ayoó de Vidriales	*Triticum sativum*	Low	9	226,89	48,24	2,13
Jun. 2016	Soto de Cerrato	*Medicago sativa*	Low	10	21,65	17,24	7,97
	San Mateo de Gallego	Triticale	High	3	50,70	70,63	13,93
	Ayoó de Vidriales	*Secale cereale*	High	3	158,00	171,91	10,88

Table 4 shows the close correspondence between the kg/ha value obtained from the field data and the value derived from photogrammetry for the different crops and plots (overall R^2=0,88 and 1,12 kg/ha), with the exception of Ayoó de Vidriales. In this plot, for 9 samples, the high irregularity of the cultivation conditions across the plot (the field sampling data ranged from a minimum of 557 kg/ha to a maximum of 11,124 kg/ha) and the low RMSE x and RMSE y values in the flight data resulted in a disparity between the results obtained from the images and from field extrapolation. With the aim of improving the intermediate volume-biomass estimation and assessing the related errors, a more extensive accuracy analysis with independent field samples could be employed in future studies.

Table 4. Overall AGB results for the test plots

Flight campaign	Plot	Crop	Density factor (kg/m^3)	Biomass field (kg/ha)	Biomass UAV (kg/ha)	Total biomass (kg)
Jun. 2013	Soto de Cerrato	*Vicia sativa*	1.41	9,85	9,89	13,56

To cite this article: ML. Gil-Docampo, M. Arza-García, J. Ortiz-Sanz, S. Martínez-Rodríguez, JL. Marcos-Robles & LF. Sánchez-Sastre (2018) Above-ground biomass estimation of arable crops using UAV-based SfM photogrammetry, Geocarto International, DOI: 10.1080/10106049.2018.1552322

	San Mateo de Gallego	*Vicia sativa*	2.63	7,11	7,16	12,70
	Ayoó de Vidriales	*Triticum sativum*	2.00	6,99	4,25	96,49
Jun. 2016	Soto de Cerrato	*Medicago sativa*	0.37	2,92	2,92	6,33
	San Mateo de Gallego	Triticale	0.21	2,92	2,97	15,07
	Ayoó de Vidriales	*Secale cereale*	0.16	1,73	1,71	27,09

4 Conclusions

In this study, we contribute to a new application of SfM photogrammetry in agronomy. Our technique can be employed to determine the AGB using an in-field calibration DF that relates volume and biomass. The proposed factor allows the B/V ratio to be generalized for the spatial extrapolation of biomass in arable crop plots. The results obtained with the proposed methodology are consistent with the biomass data collected in the field.

UAV HRV imagery is a useful source of information for biomass determination. As opposed to estimations based exclusively on sample data, the use of conventional RGB cameras mounted on drones and photogrammetric techniques allow biomass volume information to be obtained. Photogrammetry techniques with high reliability must be used to provide continuous physical quantification, whereas field data are based on the extrapolation of isolated field sampling data.

The proposed process was implemented using different platforms and sensors, and it was applied to different arable crops. The results demonstrate the satisfactory adaptability and scalability of the method. The best combination of drone type and sensor was a fixed-wing UAV with an 18-megapixel camera. Fixed-wing drones provide higher efficiency when used for large plots because they can fly the entire plot

To cite this article: ML. Gil-Docampo, M. Arza-García, J. Ortiz-Sanz, S. Martínez-Rodríguez, JL. Marcos-Robles & LF. Sánchez-Sastre (2018) Above-ground biomass estimation of arable crops using UAV-based SfM photogrammetry, Geocarto International, DOI: 10.1080/10106049.2018.1552322

in a single flight. The biomass field data support the goodness of fit of the yield-biomass estimation (kg/ha). However, a more in-depth accuracy assessment with a larger number of independent field samples could be conducted in further studies to improve the intermediate m^3/ha volume-biomass estimation, especially in plots with heterogeneous vegetation cover. Another interesting future question could involve multimodal data fusion (e.g., LIDAR, visible and NIR, thermal infrared or hyperspectral data) from UAV platforms to improve AGB estimation.

Acknowledgements

This work was supported by the life project "Operation CO_2: Integrated Agroforestry Practices and Nature Conservation Against Climate Change - LIFE+ 11 ENV/ES/535*"* and by *Xunta de Galicia* under the grant "Financial aid for the consolidation and structure of competitive units of investigation in the universities of the University Galician System (2016-18)" Ref. ED431B 2016/030 and Ref. ED341D R2016/023.

References

Becker-Reshef I, Vermote E, Lindeman M, Justice C. 2010. A generalized regression-based model for forecasting winter wheat yields in Kansas and Ukraine using MODIS data. Remote Sens Environ. 114:1312–1323.

Bendig J, Bolten A, Bennertz S, Broscheit J, Eichfuss S, Bareth G. 2014. Estimating Biomass of Barley Using Crop Surface Models (CSMs) Derived from UAV-Based RGB Imaging. Remote Sens. 6:10395–10412.

Bortolot ZJ, Wynne RH. 2005. Estimating forest biomass using small footprint LiDAR data: An individual tree-based approach that incorporates training data. ISPRS J Photogramm Remote Sens. 59:342–360.

Cooper S, Roy D, Shaaf C, Paynter I. 2017. Examination of the Potential of Terrestrial Laser Scanning and Structure-from-Motion Photogrammetry for Rapid Nondestructive Field Measurement of Grass Biomass. Remote Sens. 9:531.

Cunliffe AM, Brazier RE, Anderson K. 2016. Remote Sensing of Environment Ultra- fi ne grain landscape-scale quanti fi cation of dryland vegetation structure with drone-acquired structure-from-motion photogrammetry. Remote Sens Environ [Internet]. 183:129–143. Available from: http://dx.doi.org/10.1016/j.rse.2016.05.019

Eitel JUH, Magney TS, Vierling LA, Greaves HE, Zheng G. 2016. Remote Sensing of Environment An automated method to quantify crop height and calibrate satellite-derived biomass using hypertemporal lidar. Remote Sens Environ. 187:414–422.

Feng Z, Chen Y, Hakala T, Zhou H, Wang Y, Karjalainen M. 2018. Estimating Ground Level and Canopy Top Elevation With Airborne Microwave Profiling Radar. IEEE Trans Geosci Remote Sens.:1–12.

Fern R, Foxley E, Bruno A, Morrison M. 2018. Suitability of NDVI and OSAVI as estimators of green biomass and coverage in a semi-arid rangeland. Ecol Indic. 94:16–21.

Geipel J, Link J, Claupein W. 2014. Combined spectral and spatial modeling of corn yield based on aerial images and crop surface models acquired with an unmanned aircraft system. Remote Sens. 6:10335–10355.

To cite this article: ML. Gil-Docampo, M. Arza-García, J. Ortiz-Sanz, S. Martínez-Rodríguez, JL. Marcos-Robles & LF. Sánchez-Sastre (2018) Above-ground biomass estimation of arable crops using UAV-based SfM photogrammetry, Geocarto International, DOI: 10.1080/10106049.2018.1552322

Goldstein E, Oliver A, DeVries E, Moore L, Jass T. 2015. Ground control point requirements for structure-from-motion derived topography in low- slope coastal environments. PeerJ Prepr.

Goswami S, Gamon JA, Vargas S, Craig T. 2015. Relationships of NDVI, Biomass and Leaf Area Index (LAI) for six key plant species in Barrow, Alaska. PeerJ Prepr. 230313:1–17.

Harwin S, Lucieer A. 2012. Assessing the accuracy of georeferenced point clouds produced via multi-view stereopsis from Unmanned Aerial Vehicle (UAV) imagery. Remote Sens. 4:1573–1599.

Iqbal F, Lucieer A, Barry K, Wells R. 2017. Poppy crop height and capsule volume estimation from a single UAS flight. Remote Sens. 9.

Jimenez-Berni J, Deery D, Rozas-Larrondo P, Condon A, Rebetzke G, James R, Bovill W, Furbank R, Sirault X. 2018. High Throughput Determination of Plant Height , Ground Cover , and Above-Ground Biomass in Wheat with LiDAR. Front Plant Sci. 9:1–18.

Kachamba DJ, Ørka HO, Gobakken T, Eid T, Mwase W. 2016. Biomass Estimation Using 3D Data from Unmanned Aerial Vehicle Imagery in a Tropical Woodland. Remote Sens. 8:1–18.

Koch B. 2010. Status and future of laser scanning, synthetic aperture radar and hyperspectral remote sensing data for forest biomass assessment. ISPRS J Photogramm Remote Sens [Internet]. 65:581–590. Available from: http://dx.doi.org/10.1016/j.isprsjprs.2010.09.001

Koutsoudis A, Vidmar B, Ioannakis G, Arnaoutoglou F, Pavlidis G, Chamzas C. 2014. Multi-image 3D reconstruction data evaluation. J Cult Herit. 15:73–79.

Liu H, Zhu H, Wang P. 2017. Quantitative modelling for leaf nitrogen content of winter wheat using UAV-based hyperspectral data. Int J Remote Sens. 38:2117–2134.

Lu B, He Y. 2017. Species classification using Unmanned Aerial Vehicle (UAV) -acquired high spatial resolution imagery in a heterogeneous grassland. ISPRS J Photogramm Remote Sens. 128:73–85.

Luo S, Chen J, Wang C, Xi X, Zeng H, Peng D, Li D. 2016. Effects of LiDAR point density , sampling size and height threshold on estimation accuracy of crop biophysical parameters. Opt Express. 24:11578–11593.

Mondino EB, Gajetti M. 2017. Preliminary considerations about costs and potential market of remote sensing from UAV in the Italian viticulture context. Eur J Remote Sens. 50.

Nex F, Remondino F. 2014. UAV for 3D mapping applications: A review. Appl Geomatics. 6:1–15.

To cite this article: ML. Gil-Docampo, M. Arza-García, J. Ortiz-Sanz, S. Martínez-Rodríguez, JL. Marcos-Robles & LF. Sánchez-Sastre (2018) Above-ground biomass estimation of arable crops using UAV-based SfM photogrammetry, Geocarto International, DOI: 10.1080/10106049.2018.1552322

Qazi W, Baig S, Gilani H, Waqar M, Dhakal A, Ammar A. 2017. Comparison of forest aboveground biomass estimates from passive and active remote sensing sensors over Kayar Khola. J Appl Remote Sens. 26038–11.

Rosnell T, Honkavaara E. 2012. Point cloud generation from aerial image data acquired by a quadrocopter type micro unmanned aerial vehicle and a digital still camera. Sensors. 12:453–480.

Solberg S, Brunner A, Hanssen KH, Lange H, Næsset E, Rautiainen M, Stenberg P. 2009. Mapping LAI in a Norway spruce forest using airborne laser scanning. Remote Sens Environ [Internet]. 113:2317–2327. Available from: http://dx.doi.org/10.1016/j.rse.2009.06.010

Tonkin T, Midgley N. 2016. Ground-Control Networks for Image Based Surface Reconstruction : An Investigation of Optimum Survey Designs Using UAV Derived Imagery and Structure-from-Motion Photogrammetry. Remote Sens. 8:16–19.

Vazirabad Y, Karslioglu M. 2011. Lidar for Biomass Estimation. In: Detect Prod Usage [Internet]. [place unknown]: InTech CY; p. 3–26. Available from: http://cdn.intechopen.com/pdfs/19065/InTech-Lidar_for_biomass_estimation.pdf

Walter J, Edwards J, McDonald G, Kuchel H. 2018. Photogrammetry for the estimation of wheat biomass and harvest index. F Crop Res. 216:165–174.

Wong WVC, Tsuyuki S, Phua M, Ioki K, Takao G. 2015. Forest Biophysical Characteristics Estimation Using Digital Aerial Photogrammetry and Airborne Laser Scanning for Tropical Montane Forest. In: 36th Asian Conf Remote Sens. Quezon City, Philippines; p. 10.

Wu C, Shen H, Shen A, Dend J, Gan M, Zhu J, Xu H, Wang K. 2016. Comparison of machine-learning methods for above-ground biomass estimation based on Landsat imagery. J Appl Remote Sens. 10.

Yang S, Feng Q, Liang T, Liu B, Zhang W, Xie H. 2018. Modeling grassland above-ground biomass based on arti fi cial neural network and remote sensing in the Three-River Headwaters Region. Remote Sens Environ [Internet]. 204:448–455. Available from: https://doi.org/10.1016/j.rse.2017.10.011

Zhu X, Liu D. 2015. Improving forest aboveground biomass estimation using seasonal Landsat NDVI time-series. ISPRS J Photogramm Remote Sens. 102:222–231.

To cite this article: ML. Gil-Docampo, M. Arza-García, J. Ortiz-Sanz, S. Martínez-Rodríguez, JL. Marcos-Robles & LF. Sánchez-Sastre (2018) Above-ground biomass estimation of arable crops using UAV-based SfM photogrammetry, Geocarto International, DOI: 10.1080/10106049.2018.1552322